CHEMCOMM Communication
www.rsc.org/chemcomm

# *Z*-Contrast tomography: a technique in three-dimensional nanostructural analysis based on Rutherford scattering†

**Paul A. Midgley,[a]* Matthew Weyland,[a] John Meurig Thomas*[ab] and Brian F. G. Johnson[c]**

[a] *Department of Materials Science and Metallurgy, University of Cambridge, Pembroke Street, Cambridge, UK CB2 3QZ*
[b] *Davy Faraday Research Laboratory, Royal Institution of Great Britain, 21 Albermarle Street, London, UK W1X 4BS. E-mail: jmt@ri.ac.uk*
[c] *The University Chemical Laboratory, University of Cambridge, Lensfield Road, Cambridge, UK CB2 1EW*

***Received (in Cambridge, UK) 26th February 2001, Accepted 9th April 2001***
***First published as an Advance Article on the web***

**A method for determining the three-dimensional structure of inorganic specimens using images formed from Rutherford scattered electrons, at a spatial resolution of 1 nm in all directions, is described and illustrated with results from a study of Pd–Ru bimetallic nanocatalysts supported on mesoporous silica: a 3D animation demonstrating the results may be viewed at *http://www-hrem.msm.cam.ac.uk/~mw259/Work/Tomo.html***

Though not universally acknowledged, the electron microscope is one of the most versatile and powerful instruments for the complete chemical analysis of any solid material. Not only can it cope with sample masses ($10^{-18}$ g and less) that are far beyond the reach of X-ray analysis, it yields structural, mechanistic, compositional and electronic (valence states of ions and bonding between atoms) information on minute crystallographic phases that may contain hardly more than a dozen or so atoms. All this is possible because of the multiplicity of modes in which the microscope may be deployed. Thus it may give[1] bright field (BF) or dark field (DF) images (from forward scattered or Bragg scattered electrons, respectively) electron stimulated X-ray emission (XRE) spectra and elemental maps as well as electron energy loss spectra (EELS),[2] that can reflect such features as plasmon modes, the atomic coordination of light elements,[3] inter-atomic distances, d-electron population of transition metal ions and the momentum densities of electrons in amorphous solids.

Scanning transmission electron microscopy (STEM) is particularly useful in studies of nanoparticle catalysts supported within mesoporous silica because, by using a high angle annular dark field (HAADF) detector (see Fig. 1), which collects electrons that undergo Rutherford scattering, images can be acquired where the intensity is approximately proportional to $Z^2$ ($Z$ is the atomic number of the scattering atom).[4] Fortunately many catalytically significant elements (Pd, Pt, Ru, Re, *etc*) have high $Z$, so that when they are supported on low $Z$ material such as $SiO_2$ they are readily visible using HAADF detectors,[5] see Fig. 2. In addition the small probe sizes involved, *ca*. 0.8 nm in diameter, mean the resultant images have very high resolution. By also recording the electron-stimulated XRE from the nanoparticles their identity can be determined unambiguously (see, for example, ref. 4).

Valuable as the information yielded by STEM HAADF and XRE mapping undoubtedly is, especially in investigating nanocatalysts (and other nanoscientific problems), it is limited to providing 2D projections of 3D arrangements. The need exists to analyse, non-destructively, specimens fully in three dimensions especially if we seek to understand the factors responsible for the loss of activity, selectivity and stability of nanoparticle catalysts.

A suitable approach is electron tomography,[6] where the 3D structure is reconstructed from a tilt series of 2D projections. In practice this is achieved by tilting a specimen on one axis using the microscope goniometer and taking a micrograph at a range of tilts, typically every 1–2°, correcting for specimen move-

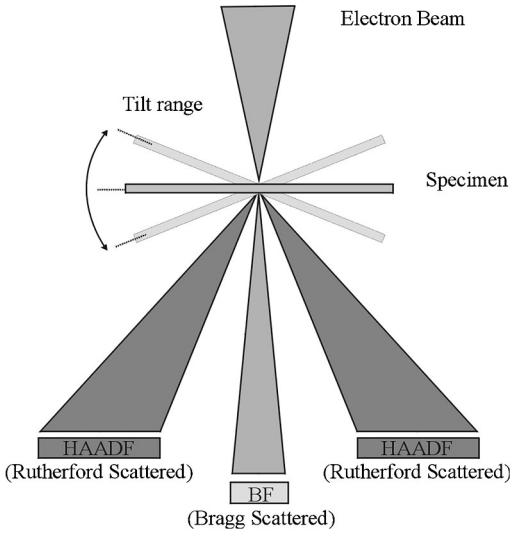


**Fig. 1** Schematic of the detector layout in a scanning transmission electron microscope (STEM). The diameter of the tip of the electron beam is 0.8 nm.

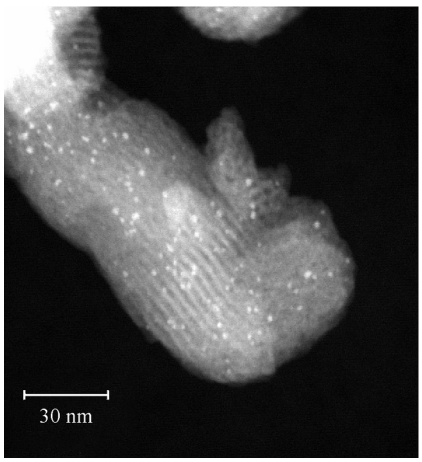


**Fig. 2** HAADF image from a Pd–Ru nanocatalyst supported on mesoporous silica and mounted on a holey carbon grid. The mesopores (3 nm in diameter) and the nanocatalyst particles (1 nm in diameter) are clearly visible.

† Electronic supplementary information (ESI) available: 3D animations of a Pd–Ru bimetallic catalyst generated from a tomographic reconstruction of HAADF STEM images. See http://www.rsc.org/suppdata/cc/b1/b101819c/

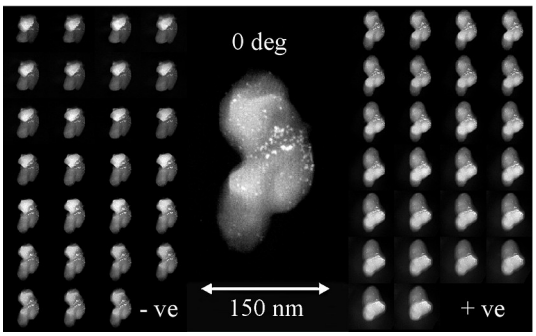


**Fig. 3** Montage of the acquired tilt series showing all images and an enlargement of the zero tilt image.

ment, focus change and astigmatism throughout. In our case, the series is then processed offline using routines based on the Radon Fourier-slice theorem,[7] to reconstruct the full 3D structure.

In conventional electron tomography such a series is acquired using BF images dominated by Bragg-scattered electrons.[6] However, the large beam currents of conventional TEM means that such an approach cannot be used on specimens that are beam sensitive. The framework structure of mesoporous silica, for example, degenerates rather rapidly under TEM illumination and so is unsuitable for the prolonged acquisition times required for a tilt series. By using STEM, however, far smaller total beam exposure is involved. (Although the current density within the STEM probe is high, its energy can be dissipated to the surrounding (non-illuminated) areas unlike conventional static beam TEM). Another advantage arises from the scattering geometry in that HAADF imaging excludes almost all the electrons scattered coherently through low angles. This means that the resulting images are free from the misleading complications of electron phase contrast and, as such, they are 'true-projections' of the structure. As HAADF STEM images are formed primarily from incoherently scattered electrons, the combination of STEM HAADF imaging coupled with high operating voltages, to minimise inelastic interactions and thus ionisation damage, is an ideal basis for the tomography of catalysts.

We illustrate the power of HAADF STEM tomography by examining Pd–Ru bimetallic catalysts[8] supported on mesoporous silica. A HAADF tilt series was acquired on a CM300 field emission gun transmission electron microscope (FEGTEM), operating at 300 kV, in STEM mode using an on-axis Fischione HAADF detector. The series was acquired from +60° to −48° with an image every 2° giving a total of 55 images. These were spatially aligned using a cross-correlation algorithm applied sequentially to images stretched using an inverse cosine function that takes into account the variation in image width with tilt. After determining the tilt-axis for the data set, a 3D reconstruction was achieved using a weighted back-projection of consecutive 2D slices.[6a] The additional weighting function corrects for the relative oversampling of low frequencies when combining the image series from successive tilts.[6a]

The resultant reconstructions[9] have been displayed using multi-level voxel[10] projections, see Fig. 3. The multi-level voxel projection is achieved by contrast-selecting intensities from the reconstruction and assigning them definite colour and opacity values. This allows clear differentiation between the silica support (coloured grey) which has low intensity in the reconstruction from the low $Z$ $SiO_2$, and the active nanoparticles (coloured red) which have high intensity in the reconstruction due to the high $Z$ of the Pd/Ru. The reconstruction has sufficient resolution (1 $nm^3$) to allow a direct visualisation of the relative positions of mesopores and nanoparticles in all directions. Here we can show only 2D projections, but for the full 3D picture the reader may view an animation in the supplementary information (ESI†) on the RSC web site or at our web site.[11]

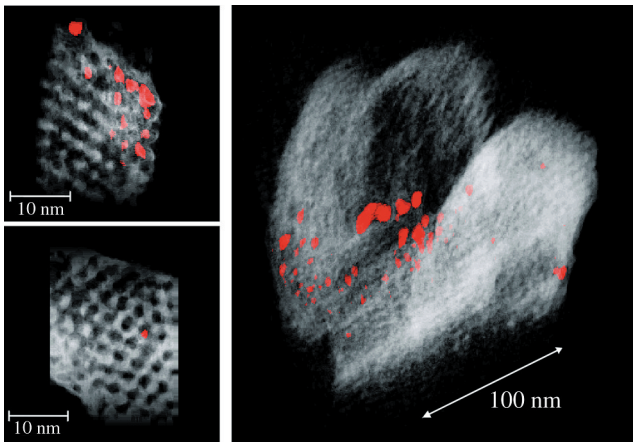


**Fig. 4** Results from the tomographic reconstruction from the tilt series in Fig. 3. All images are multi-level voxel[10] red, green, blue, opacity (RGBO) projections. (a) and (b) are regions selected from the full reconstruction and (c) illustrates the reconstruction of nanoparticles and channels in multiple directions. The Pd–Ru particles are coloured red in all figures.

The reconstruction, as seen here or with the animations, reveals a number of important factors. On a practical level, it is clear that the silica framework has been reconstructed faithfully with essentially no beam damage even though long acquisition times are needed for the full series. The nanoparticles have a clear size distribution with larger particles sitting on the outside of the silica and smaller ones within the silica channels. The larger particles are those in which the original $Pd_6Ru_6$ metal clusters have coalesced. Those that have diameters $>3$ nm cannot be incorporated into the silica framework without severe disruption. Fig. 4(b) and the accompanying animation show a single nanoparticle anchored to the side of the wall of the silica channel exactly as suspected from other studies.[8] It is this type of nanoscale structural information, retrieved by non-destructive methods in contrast to atom-probe tomography,[12] coupled with bulk chemical analysis, which will be invaluable in developing and evaluating catalysts in the future.

Although we have demonstrated this technique primarily for the purposes of characterising supported catalysts, it has patently wide applications across the entire corpus of nanoscience and nanotechnology.

We acknowledge with thanks continued support from EPSRC (rolling grant to J. M. T.) and BNFL Research and Technology (studentship for M. W.).

## Notes and references

1 J. M. Thomas, in *Inorganic Chemistry: Towards the 21st century*, ed M. H. Chisholm, ACS Publication 211, Washington, DC, 1983, p. 445.
2 J. M. Thomas, B. G. Willimas and T. G. Sparrow, *Acc. Chem. Res.*, 1985, **18**, 324.
3 R. D. Brydson, J. M. Thomas, H. Saur, W. Engel and E. Zeitler, *J. Chem. Soc., Chem. Commun.*, 1989, **15**, 1010.
4 D. Ozkaya, W. Zhou, J. M. Thomas, P. A. Midgley, V. J. Keast and S. Hermans, *Catal. Lett.*, 1999, **60**, 101.
5 M. M. J. Treacy and A. Howie, *J. Catal.*, 1980, **63**, 265.
6 (*a*) *Electron Tomography*, ed. J. Frank, Plenum Press, New York, 1992; (*b*) A. J. Koster, U. Ziese, A. J. Verkleij, A. H. Janssen and K. P. de Jong, *J. Phys. Chem. B*, 2000 **104**, 9368.
7 S. R. Deans, *The Radon Transform and Some of Its Applications*, John Wiley & Sons, New York, 1983.
8 (*a*) R. Raja, G. Sankar, S. Hermans, D. S. Shephard, T. Maschmeyer, S. Bromley, J. M. Thomas and B. F. G. Johnson, *Chem. Commun.*, 1999, **16**, 1571; (*b*) J. M. Thomas, *Angew Chem., Int. Ed.*, 1999, **38**, 3588.
9 All processing was undertaken using routines programmed in the IDL image processing language running on an IRIX operating system.
10 Voxel = a three dimensional pixel.
11 Department of Materials Science and Metallurgy Electron Microscopy Group: *http://www-hrem.msm.cam.ac.uk/~mw259/Work/Tomo.html*
12 M. K. Miller, *Atom-Probe Tomography: Analysis at the Atomic Level*, Kluwer Academic/Plenum Press, New York, 2000.